JOURNAL OF MATERIALS SCIENCE 14 (1979) 1071–1079

On the intergranular fracture mechanism due to ledge formation in an Al–6.0% Zn –2.5% Mg alloy

TAKESHI KAWABATA, OSAMU IZUMI
The Research Institute for Iron, Steel and Other Metals, Tohoku University, Sendai, 980, Japan

The ledges observed on the over-load fracture surfaces of an Al–6.0% Zn–2.5% Mg alloy variously heat treated are discussed. As pointed out by Ryum and Baardseth the ledges are formed by the reaction between slip bands and grain boundaries. The morphology of the ledges changes from a sharp saw-toothed to a sine-curved shape, and the facets of the ledges vary from a flat face to a dimpled one with the degree of ageing. Grain-boundary precipitates were frequently observed on the flat facets. The fracture stress, calculated from a modified equation of Stroh's theory, supports the possibility of fracture occurring at a stress a little beyond yielding.

1. Introduction

It is well-known that fracture of high strength Al–Zn–Mg alloys occurs predominantly at grain boundaries (GB) [1, 2]. Two kinds of microstructure, i.e. (i) dimples and (ii) straight stair-like waves (or ledges), on the fracture surface of Al–Zn–Mg alloys have been observed. Usually, the dimples are more observable on fracture surfaces as reported previously [3], and they are attributed to the evidence that fracture occurred by the nucleation, growth and coalescence of voids (void formation mechanism). Concerning the ledges, there has been only one short communication by Ryum and Baardseth [4]. They proposed that the ledges resulted from the pile ups of dislocations to the GB.

In the present investigation, evidence will be presented that GB fracture due to ledge formation occurs in an Al–Zn–Mg alloy under wide ageing conditions, the morphology of ledges will be classified by ageing conditions, and the fracture stress on the mechanism of ledge formation will be estimated.

2. Experimental procedures

The chemical composition of the specimens was Zn: 6.0, Mg: 2.5, other minor impurity elements Fe, Si, Cu < 0.01 wt %, and Al: remainder. Single-notched tensile specimens with side-grooves having a nominal sectional area 1.5×10^{-2} m $\times$ 4.0×10^{-2} m were used. After being solution treated at 733 K for 3 h, the specimens were interrupt-quenched at 613 K for x sec, and quenched into iced water, and immediately two-step-aged at 373 and 433 K for y sec and z h, respectively. At the front of the notch, a fatigue crack was introduced by superimposing supersonic vibrations to a slight bending stress. The electric tube-type universal testing machine was used for the tensile test at nearly constant loading rate, $\simeq 2000$ N min^{-1}. Fracture surfaces were observed by a scanning electron microscope (JSM-U3).

3. Experimental results and discussions

3.1. Evidence of ledge formation

Fig. 1a to h shows ledges observed on the intergranular fracture surface of specimens heat-treated variously. The experimental evidence for ledge formation on fracture surfaces is as follows:*

(1) the ledges are parallel to each other and are aligned regularly at nearly the same interval;

(2) there are some cases where two or more groups of ledges intercept each other and a compli-

*The ledges were observed at a random site of fracture surface not only in the notched tensile specimens but also in the unnotched tensile specimens.

© 1979 Chapman and Hall Ltd. Printed in Great Britain.

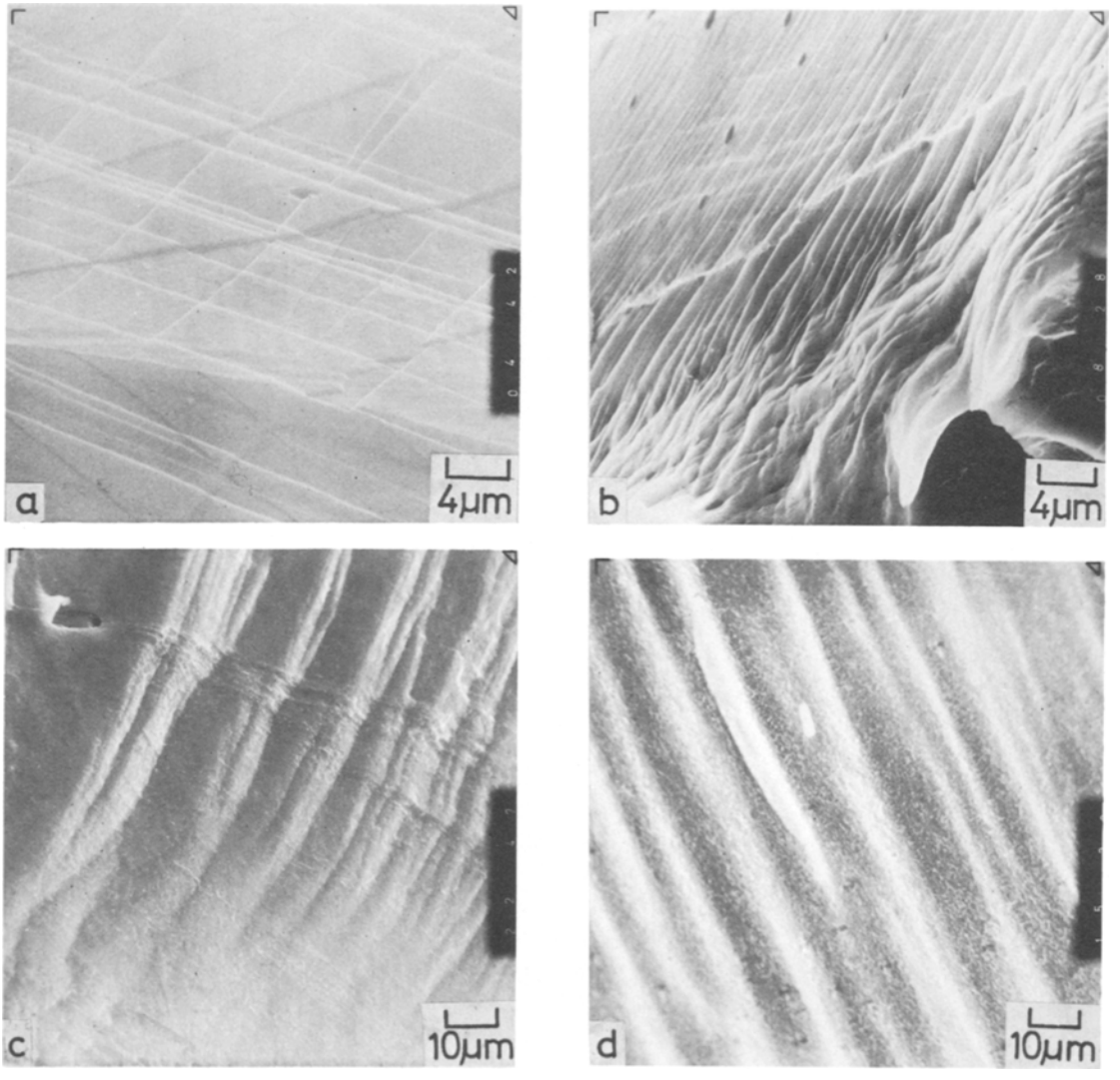

Figure 1 Morphologies of ledges on fracture surfaces of an Al–6.0% Zn–2.5% Mg alloy subjected to various heat-treatments. (a) As-quenched, (b) aged at 373 K for 4 h, (c) aged at 433 K for 4 h, (d) aged at 433 K for 70 h, (e) pre-aged at 373 K for 300 sec and subsequently aged at 433 K for 3.5 h, (f) pre-aged at 373 K for 3000 sec and subsequently aged at 433 K for 3.5 h, (g) pre-aged at 373 K for 3×10^5 sec and subsequently aged at 433 K for 2 h, after solution-treatment at 733 K for 3 h, (h) solution-treated at 733 K for 4 h, interrupt-quenched at 613 K for 30 sec and quenched into iced water, and then aged at 433 K for 4 h.

cated and straight-line geometrical pattern is formed;

(3) facets of the ledges on fracture surface are comparatively smooth and dimples are not observed on the facets except under some ageing conditions (e.g. except the longer interrupted quenching treatment and the ageing at higher temperature);

(4) there are some cases where many GB precipitates are observed on the flat surfaces.

These indicate that intergranular fracture is not only caused by void formation but also by ledge formation.

3.2. Classification of ledge morphology

Features of the ledges can be classified into five groups corresponding to ageing conditions. Fig. 2a to e shows these features. Fig. 2a shows as-quenched or incompletely aged material: ledges have sharp edges and are of a saw-toothed shape.

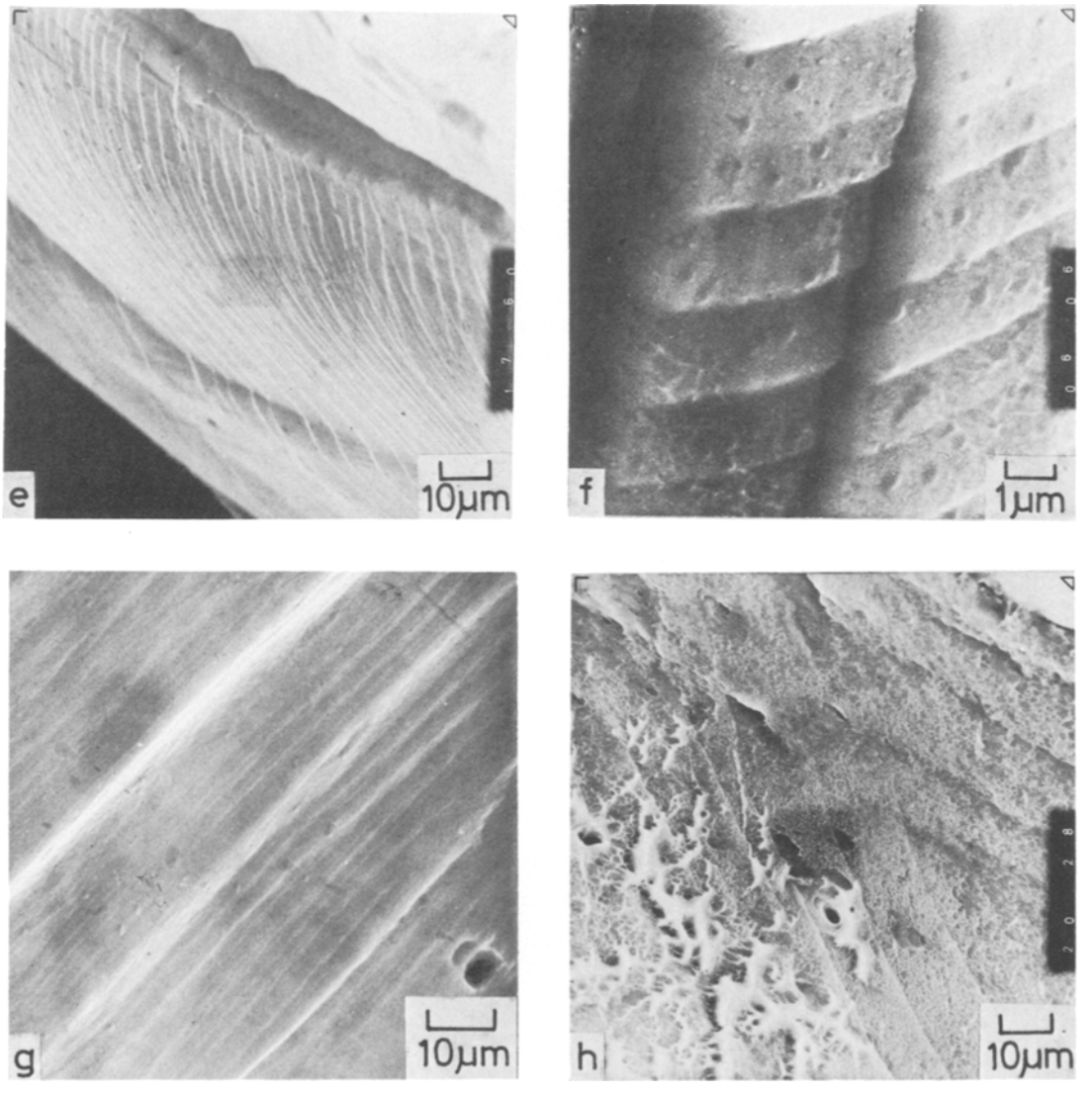

Figure 1 continued.

With increasing ageing period, the sharpness of the ledges decreases and the shape of the ledges changes to wavy facets (Fig. 2b). Fig. 2c shows material fully aged to the highest hardness: the wavy shape changes to an easy sine curve. Over-aged material is shown in Fig. 2d: Micro-dimple patterns are superimposed on the sine curved ledges. In other cases, many fine GB precipitates were also observed on the smooth sine-curved ledges. Fig. 2e shows the ledge observed in the specimen which was subjected to a longer interrupted quenching and over-ageing. The ledges are again sharpened as in the as-quenched specimen, and highly ductile dimples are observed on the fracture surface.

3.3. Mechanism of ledge formation

Fig. 3a to d shows transmission electron micrographs of deformed specimens. Fig. 3a is a micrograph at low magnification. It is observed that coarse slip bands traverse the grain. From Fig. 2b it is not clear whether or not the shape of the slip bands in PFZ is the same as in the grain interior. In this case there was no evidence that dislocations were active along the GB in PFZ, i.e. dislocation structure was not observed in PFZ. Fig. 3c and d are micrographs showing the dislocation arrangement in the slip bands. The dislocations in the slip bands pile up with complex morphology, and no dislocation exists between the slip bands. The features of the deformed microstructure are in

good agreement with those of Hall [5], Ryum and co-workers [6, 7] and Sedriks *et al.* [8].

From the above observations of fracture surfaces using a scanning electron microscope and of the deformed microstructure using a transmission electron microscope, it is deduced that the fracture due to the formation of GB ledges occurs through the following process; (1) the leading dislocation in a slip band reacts with the GB because the GB is considered as a layer with a lower Young's modulus than the matrix, and the leading dislocation forms a ledge with the height of $\boldsymbol{b}$ on the interface belonging to one side of the grains, where $\boldsymbol{b}$ is the Burgers vector, and a wedge-shaped GB microcrack is formed on the tension side of ledge; (2) the ledge height, which is as large as $\boldsymbol{b}$, grows to $n\cdot\boldsymbol{b}$ by absorbing the following $(n-1)$ dislocations and at the same time the length of the wedge-shaped crack increases; (3) when the ledge height $n\cdot\boldsymbol{b}$ reaches $n_c\cdot\boldsymbol{b}$ (n_c: the critical number of dislocations for growing to a macroscopic crack) and the crack length, l, becomes as long as the ledge distance (l_c) the microcracks formed at each ledge begin to coalesce with each other and grow to a macrocrack. The experimental evidence already described in Section 3.1 can be explained reasonably by a decohesion mechanism of the GB due to ledge formation, as presented above.

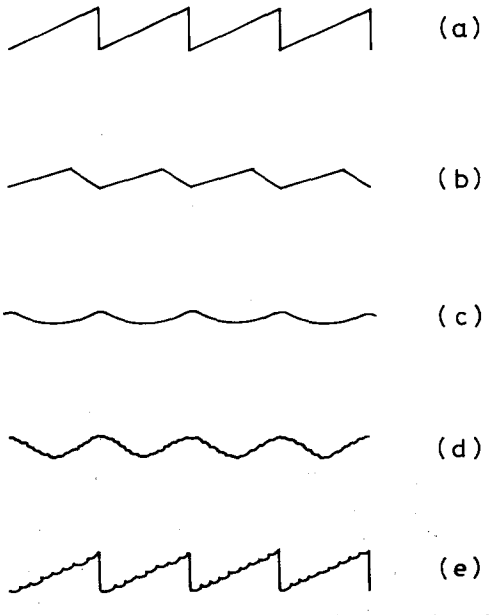

Figure 2 Classification of morphology of ledges changed by ageing conditions in an Al–Zn–Mg alloy. (a) and (b) as-quenched and incompletely aged material, respectively, (c) fully aged to the highest hardness, (d) over-aged material, and (e) longer interrupt-quenched and over-aged materials.

3.4. Variation of ledge morphology due to ageing conditions

Fig. 4 shows schematically the variation of ledge morphology with width of the deformation band. In as-quenched or incompletely aged conditions, the microstructure contains small Guinier–Preston zones and/or small η' precipitates [9–11]. Therefore, dislocations can move by cutting those zones and/or precipitates. As a result, the width of deformation bands becomes narrow [12] and then the ledge becomes sharp (saw-toothed ledge: Fig. 4a and b). Naturally the morphology of the ledge also changes due to the angle of the slip band to the GB. According to Stroh [13], the tensile stress at the front of pile-ups reaches a maximum on a plane inclined $\sim 70.5°$ to the slip plane so that there is a tendency for the ledge to become sharp. Fig. 4c and d show a case in which the slip band is wide. Each slip plane in a slip band forms many steps on the GB; therefore, one slip band forms one ledge inclined obtusely as shown in Fig. 4d, and, macroscopically, a wavy fracture surface results.

The size of the precipitates becomes larger with increasing ageing period, and then the cutting of precipitates due to dislocations becomes more difficult. Thus, the probability of cross-slip occurring near the large precipitates will increase so that the width of the slip band becomes wide. At the over-aged condition, the size of the precipitates increases and the number of precipitates decreases so that dislocations cannot cut the precipitates but by-pass them due to the Orowan mechanism. Therefore, the width of the slip band again becomes narrow.

There also exists some evidence of GB fracture due to ledge formation in other metals and alloys. Kovacs and Low [14] observed ledges similar to that in Fig. 2b in Al–15% Zn alloy. Most recently Dunwoody *et al.* [15] also observed similar ledges on the intergranular fracture surface of Al–Mg–Si alloy by scanning electron microscopy.

3.5. Estimation of fracture stress due to ledge formation

Consider that a number $(N-1)$ of dislocations which are freely movable on a slip plane, pile up behind the leading dislocation impeded in its motion by an obstacle such as a GB. According to

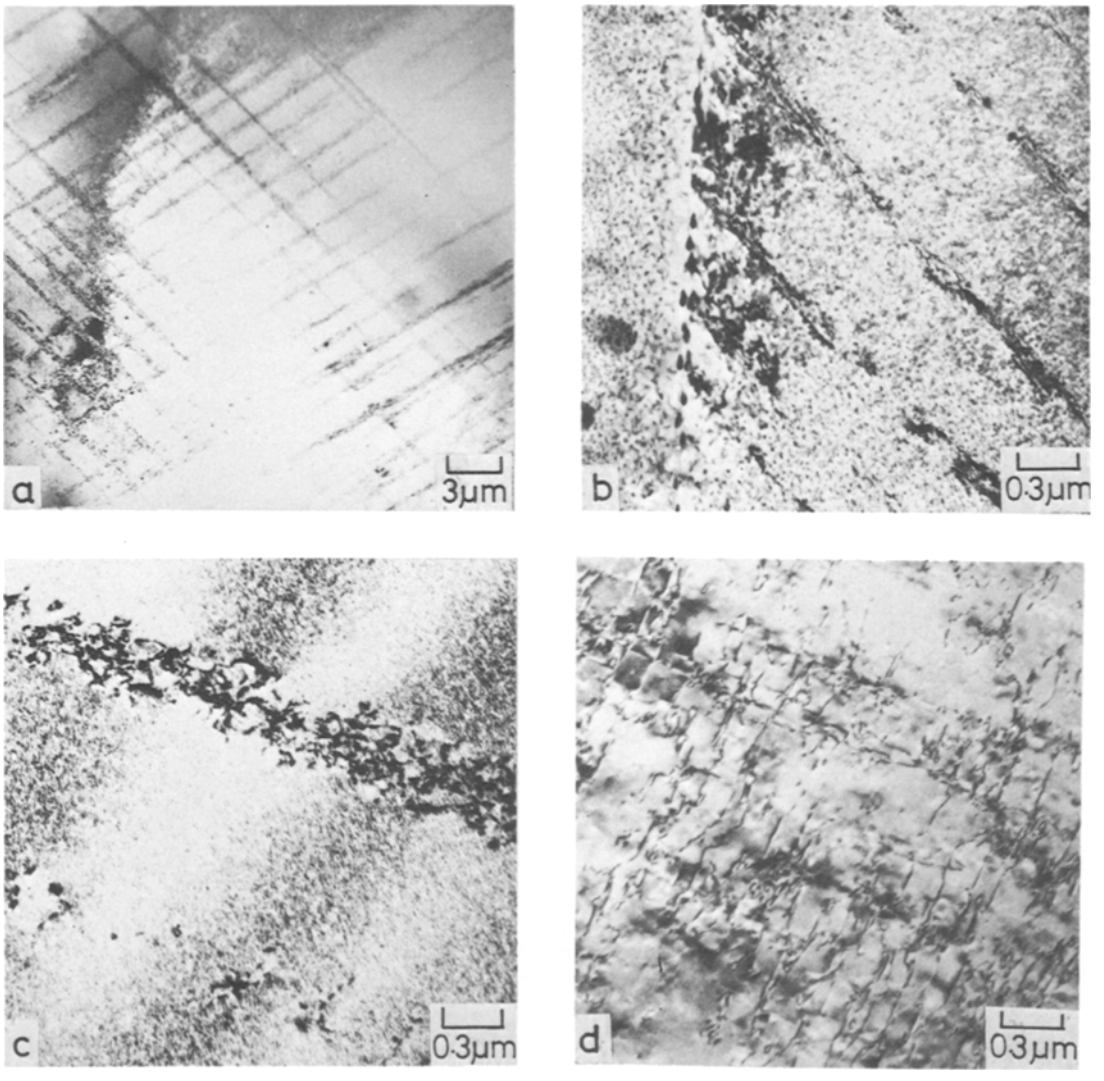

Figure 3 Transmission electron micrographs of thin foils made from deformed specimens.

Stroh [13], the normal stress, σ, near the leading dislocation is expressed as follows,

$$\sigma = \frac{3}{2}\left[\frac{L}{r}\right]^{1/2} \tau_e \cdot \sin\theta \cdot \cos\frac{\theta}{2} \qquad (1)$$

where L is the pile-up length of dislocations, i.e. a half of grain size, r the distance of point P from the position of the leading dislocation expressed in the polar co-ordinates, τ_e the effective shear stress, θ the angle between the plane applied tensile stress and the slip plane. The plane of the applied tensile stress is coincident with the line linking the point P with the origin O. This relationship is shown in Fig. 5.

Furthermore, when a slip band consists of M slip planes aligned at an interval s, the tensile stress at the point y on the GB is expressed as the summation of stresses from each slip plane, based on the assumption that the interaction between dislocations on different slip planes can be neglected and that the relationship between stress and strain is linear, i.e. stresses and strains from each dislocation can be simply summed up. That is,

$$\sigma = \sum_{k=0}^{M-1} \frac{3}{2}\frac{(y-k\cdot s)}{|y-k\cdot s|}\left[\frac{L}{|y-k\cdot s|}\right]^{1/2} \cdot \tau_e \cdot \sin\theta \cdot \cos\frac{\theta}{2}. \qquad (2)$$

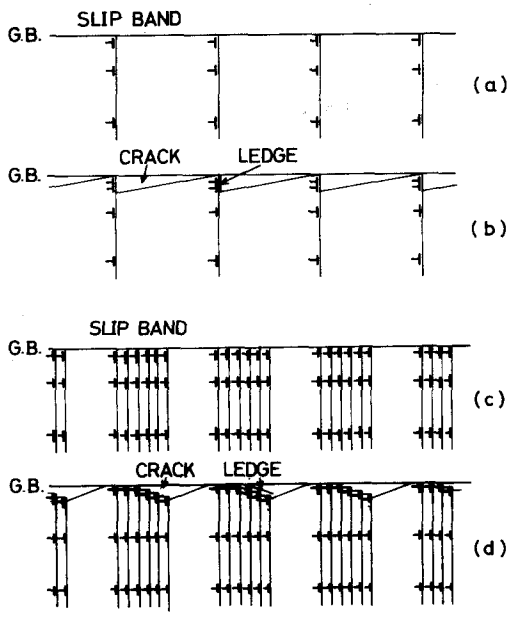

Figure 4 Schematic drawings explaining the differences in ledge morphology with width of slip band. (a) and (b) show one slip band constructed from one slip plane, (c) and (d) show a slip band constructed from many slip planes.

The energy criterion for the formation of a crack is confirmed from Stroh's calculation [13] as follows, when the slip band is constructed by a single slip plane,

$$N\tau_e > \frac{64}{9}\frac{\alpha G}{\sin^2\theta\cdot\cos^2(\theta/2)}, \tag{3}$$

where G is the shear modulus, N the number of piled up dislocations, τ_e the effective shear stress, $\alpha = \gamma_s/(bG) \simeq 0.06$, γ_s the surface energy and b the Burgers vector [13]. Now, we consider that fracture occurs at a GB (i.e. separation of a GB) so that α in the above equation must be substituted by α'

$$\alpha' = \frac{(\frac{1}{2})\gamma_f}{bG} = \frac{1}{2}\frac{\gamma_s}{bG}\left(2 - \frac{\gamma_{gb}}{\gamma_s}\right), \tag{4}$$

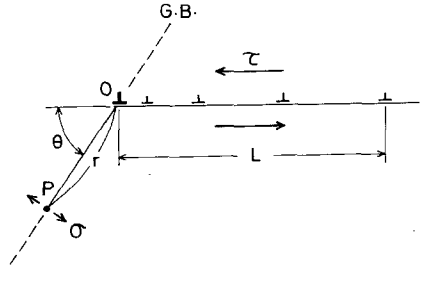

Figure 5 A schematic drawing of piled-up dislocations impeded by a grain boundary.

where γ_f is the energy needed to cause GB fracture and is related to the surface energy, γ_s, and the GB energy, γ_{gb}.

Generally in f c c metals [16], $\gamma_{gb}/\gamma_s \simeq 0.35$, so that $\alpha' \simeq 0.0495$.

There exists a relationship between τ_e and N as follows [17],

$$\tau_e = \frac{4A}{L_g}\cdot N, \tag{5}$$

where L_g is the grain size (i.e. twice the pile-up length) and

$$A = \frac{Gb}{2\pi(1-\nu)}. \tag{6}$$

When the energy criterion is satisfied, combining Equations 3, 5 and 6, and replacing α with α', the critical number of piled-up dislocation, N_c, is found as follows:

$$N_c = \frac{4}{3}\frac{1}{\sin\theta\cdot\cos(\theta/2)}\left[\frac{2\pi(1-\nu)\alpha'}{b}\right]^{1/2}\cdot L_g^{1/2}. \tag{7}$$

Then, the critical effective stress, τ_{ec}, is

$$\tau_{ec} = \frac{16}{3}\frac{G}{\sin\theta\cdot\cos(\theta/2)}\left[\frac{\alpha' b}{2\pi(1-\nu)}\right]^{1/2}\cdot L_g^{-1/2}; \tag{8}$$

τ_{ec} is represented by the critical actual applied stress (i.e. the fracture stress), τ_f, and the frictional stress, τ_i, in which all frictions, against the motion of dislocations due to solute atoms and precipitates, etc., are contained. Therefore,

$$\left.\begin{aligned} &\tau_f = \tau_i + k_e\cdot L_g^{-1/2} \\ &\text{where,} \\ &k_e = \frac{16}{3}\cdot\frac{G}{\sin\theta\cdot\cos(\theta/2)}\cdot\left[\frac{\alpha' b}{2\pi(1-\nu)}\right]^{1/2}. \end{aligned}\right\} \tag{9}$$

This equation expresses the grain-size dependence of the fracture stress which obeys the energy criterion when intergranular fracture occurs due to ledge formation.

The initiation of fracture cannot merely be prescribed by the energy criterion of the fracture obtained from comparing the formation energies of a slip band and a crack, because it needs to overcome an energy barrier during the state change even if the formation of a crack makes the system

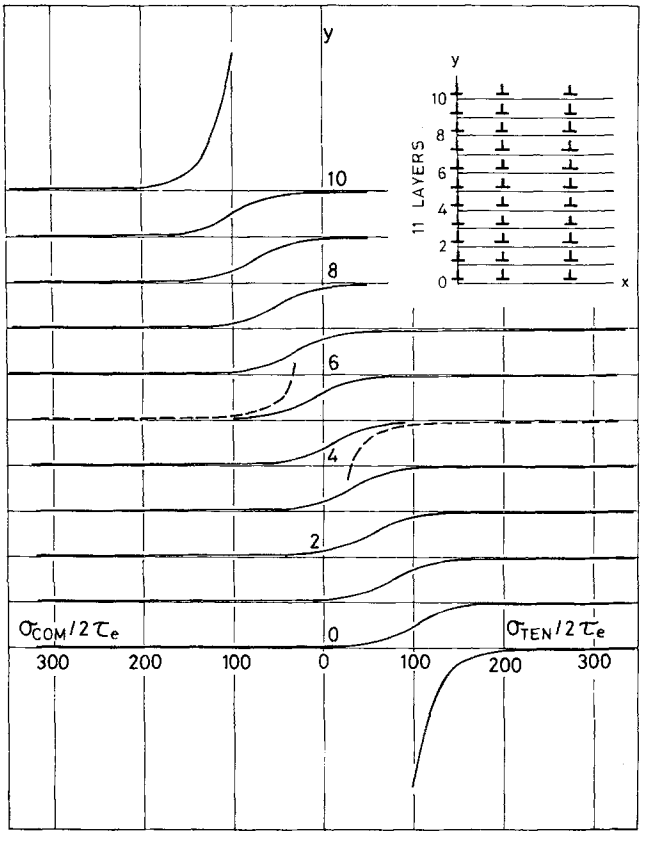

Figure 6 The stress distributions at the front of a slip band constructed from a single and eleven slip planes, represented by the dotted and solid lines, respectively.

more stable energetically. At present the barrier is considered to be the maximum repulsion force between the leading and the second dislocations when they combine with each other.

According to Stroh [18], a small crack exists at the tensile side around the leading dislocation, and then the repulsion force, F, between the leading and the second dislocations is expressed by x which is the distance between dislocations and is small compared with the length of the crack as follows,

$$F = \tfrac{1}{2}bA\left[(2xC_o)^{-1/2} - \tfrac{1}{2}x^{-1}\right] \qquad (10)$$

where

$$C_o = \frac{Gb^2}{8\pi(1-\nu)\gamma_s}. \qquad (11)$$

The dislocation on a GB has a small crack, so that replacing γ_s with $\gamma_f/2$, one finds

$$C_o' = \frac{Gb^2}{4\pi(1-\nu)\gamma_f}. \qquad (11)'$$

When one dislocation approaches a crack which is formed by combining n dislocations, the force can also be expressed by the same equation. However, Stroh has deduced that C_o takes the large value of 4 er_o when n is small, where r_o is the core radius of dislocation, and with increasing n, C_o comes to obey Equation 11. Therefore, F changes with C_o, i.e. F is small when initially two dislocations combine and becomes large with increasing n.

Stroh [18] has shown that the maximum force for the combination of two dislocations is $F_{max} = 0.28\,(bA/C_o)$. When the second dislocation combines with the leading dislocation or crack, the force condition is

$$(N-1)\tau_e > 0.28\,\frac{A}{C_o}. \qquad (12)$$

When $N \gg 1$, from Equations 5, 6, 11′ and 12, N_c for the combination of dislocations or for the formation of a crack is,

$$N_c = \left[0.56\cdot\frac{\pi(1-\nu)\alpha'}{b}\right]^{1/2}\cdot L_g^{1/2}. \qquad (13)$$

Then similarly in Equations 8 and 9 τ_{ec} and τ_f are given as follows,

$$\tau_{ec} = \left[2.24\cdot\frac{\alpha' bG^2}{\pi(1-\nu)}\right]^{1/2}\cdot L_g^{-1/2}. \qquad (14)$$

where,

$$\left.\begin{aligned} \tau_f &= \tau_i + k_f L_g^{-1/2} \\ k_f &= \left[2.24 \cdot \frac{\alpha' b G^2}{\pi(1-\nu)}\right]^{1/2} \end{aligned}\right\} \quad (15)$$

These equations express the grain-size dependence of the fracture stress which obeys the force condition when intergranular fracture occurs due to ledge formation. By comparing the force Equation 14 with the energy Equation 8 we realize that the effective stress for the formation of a crack in accordance with the force equation is nominally about $\frac{1}{13}$ of that in the energy equation. Actually the applied effective stress becomes about 0.28 times because the decrease of the applied effective stress associates with the decrease of the number of piled up dislocations.

At first we considered the combination of dislocations as a barrier but now we recognize that the incorporation of dislocations occurs more easily than the condition given by the energy criterion. In the energy criterion the energies of a crack formed by the combination of n dislocations and a slip band with the same number of dislocations have been compared without considering any process for the change of state. In the force condition, we considered a state that dislocations combine and then the leading dislocation pushed by the following $(N-1)$ dislocations is absorbed into a crack formed by combining n dislocations. As the following dislocations are absorbed into the crack, in turn, the same number or more of dislocations are nucleated additionally on the slip plane, because the applied stress is increased with the growth of the crack. Therefore, growth of the crack is always helped by a stress concentration of piled-up dislocations.

When (i) a slip band is made from one slip plane under the condition $\theta = 90°$, and (ii) the material parameters are assumed to be $L_g = 2 \times 10^{-4}$ m, $b = 2.86 \times 10^{-10}$ m, $G = 2.45 \times 10^4$ MN m^{-2} and $\nu = 0.33$ [19], the combination of the pile-up dislocations forming a crack on a GB leads to $N_c = 202$ and $\tau_{ec} = 6.73$ MN m^{-2} for the force condition, and $N_c = 720$ and $\tau_{ec} = 24.0$ MN m^{-2} for the energy condition.

The above results show that there exists a possibility of fracture due to ledge formation, and the separation of a GB occurs at a small stress over the yield stress, i.e. within a small strain after yielding. In practice, the work-hardening rate of high strength Al–Zn–Mg alloy is not as large as the ultimate tensile stress, i.e. the stress–strain curve after yielding is nearly flat. As discussed elsewhere [2], the dimple fracture predominantly occurs in this alloy by the void formation within PFZ, associated with shearing deformation along the GB. However, if there is a GB, to which dislocations pile-up, intergranular fracture may occur by ledge formation. Based on the difference between the ledge and the dimple fracture mechanisms, it is found that dimple fracture occurs usually at a lower stress level than ledge formation fracture. This deduction agrees with the experimental results that GB fracture due to ledge formation was observed on specimens variously heat-treated, although it was not predominant.

We then compare the two cases of stress at the GB; the case of a slip band consisting of one single slip plane, and the case of M slip planes. For simplification we assume that the number of piled-up dislocations in a slip plane is the same in the two cases (e.g. $N = 202$, $\tau = 6.73$ MN m^{-2}). Fig. 6 shows the distribution of normal stress on the GB of a slip band constructed from a single slip plane and eleven slip planes piled up to a GB at $\theta = 90°$. At the right-hand side of the upper part of the figure, a scheme of piled-up dislocations is shown. $0x$, $0y$ and the numbers 0 to 10 represent the first slip plane, the GB and the number of slip planes, respectively. The stress distribution on the GB due to the slip band constructed from a single slip plane is drawn by a dotted line at the position of the fifth slip plane. The vertical axis is the position of each slip plane and the horizontal axis is the ratio of normal stress (σ_{tens}, σ_{comp}: the tensile and compressive stresses, respectively) to $2\tau_e$. From these curves, it is recognized that the stress near the y-axis in the middle of the slip band constructed from M slip planes is nearly equal to that constructed from a single slip plane and the stress levels of either compression or tension increase when approaching the upper and lower slip planes. The maximum tensile stress is obtained at the first slip plane of the lower part. Therefore, it is deduced that the initiation of intergranular cracking at the front of the slip band composed of M slip planes begins at the first slip plane of the lower part, and the level of the effective applied stress is far smaller than that of a single slip plane.

4. Conclusions

The experimental results of the ledges rarely observed on the fracture surface of an Al–Zn–Mg

alloy variously heat-treated are shown and the conditions for the ledge formation were discussed.

(1) As pointed out by Ryum, the ledges are formed due to the reaction between the slip band and the grain boundary, and then the fracture by the separation of the grain boundary itself occurs.

(2) The morphology of the ledges varies from a sharp saw-toothed to a sine-curved shape with the degree of ageing. This change is related to the width of the slip band.

(3) In the over-aged condition, both ledges and dimples are observed. This was considered to be fracture caused by ledge formation after the initiation of microvoids.

(4) A modified form of Stroh's theory, which was obtained from the energy balance and the force balance between dislocations or a crack and dislocations, explains the fracture due to the separation of the grain boundary, and the applied stresses for the initiation of fracture were calculated. According to these calculations there exists a possibility that fracture may even occur at a stress level only a little higher than the yield stress.

Acknowledgements

The authors wish to express appreciation to Drs E. Hata and Y. Baba in the Sumitomo Light Metal Industry, Ltd for the supply of materials, and Emeritus Professor S. Shimodaira and Mr T. Sato for the use of the scanning electron microscope. This work was supported partly by the Keikinzoku Shogakukai (The Light Metal Educational Foundation, Incorporated) and Grant-in Aids for Fundamental Scientific Research from the Ministry of Education.

References

1. P. N. T. UNWIN and G. C. SMITH, *J. Inst. Metals* **97** (1969) 299.
2. T. KAWABATA and O. IZUMI, *J. Mater. Sci.* **11** (1976) 892; *Acta Met.* **24** (1976) 817.
3. D. A. RYDER and A. C. SMALE, "Fracture of Solids", edited by D. C. Drucker and J. J. Gilman (Interscience, New York, 1963) p. 237.
4. N. RYUM and K. BAARDSETH, *J. Inst. Metals* **96** (1968) 92.
5. H. A. HALL, *Corrosion* **23** (1967) 173.
6. N. RYUM, B. HAEGLAND and T. LINDTVEIT, *Z. Metallk.* **58** (1967) 28.
7. N. RYUM, *Acta Met.* **16** (1968) 327.
8. A. J. SEDRIKS, P. W. SLATTERY and E. N. PUGH, *Trans. ASM* **62** (1969) 815.
9. G. THOMAS and J. NUTTING, *J. Inst. Metals* **88** (1959/60) 81.
10. J. D. EMBURY and R. B. NICHOLSON, *Acta Met.* **13** (1965) 403.
11. J. GJØNNES and C. J. SIMENSEN, *ibid* **18** (1970) 881.
12. N. RYUM, *ibid* **17** (1969) 821.
13. A. N. STROH, *Proc. Roy. Soc.* **A223** (1954) 404.
14. W. J. KOVACS and J. R. LOW Jr, *Met. Trans.* **2** (1971) 3385.
15. B. J. DUNWOODY, D. M. MOORE and A. T. THOMAS, *J. Inst. Metals* **101** (1973) 172.
16. R. A. SWALIN, "Thermodynamics of Solids", 2nd Edn. (Wiley, New York, 1972) p. 247.
17. J. D. ESHELBY, F. C. FRANK and F. R. N. NABARRO, *Phil. Mag.* **42** (1951) 351.
18. A. N. STROH, *Proc. Roy. Soc.* **A232** (1955) 548.
19. L. F. MONDOLFO, "The Aluminum–Magnesium–Zinc Alloys", Research and Development Center, Revere Copper and Brass Incorporated, Rome, New York (1967) p. 171.

Received 8 May and accepted 4 October 1978.